Vacuum 165 (2019) 290–296

Contents lists available at ScienceDirect

Vacuum

journal homepage: www.elsevier.com/locate/vacuum

Nanorods of ZnO: An effective hydrazine sensor and their chemical properties

Rizwan Wahab[a,*], Naushad Ahmad[b], Manawwer Alam[b], Javed Ahmad[a]

[a] Zoology Department, College of Science King Saud University, Riyadh, 11451, Saudi Arabia
[b] Department of Chemistry, College of Science, King Saud University, P.O. Box 2455, Riyadh, 11451, Saudi Arabia

ARTICLE INFO

Keywords:
ZnONRs
Hydrazine
Amperometry
Nyquist plot

ABSTRACT

In this paper, ZnO nanorods (ZnONRs) have been synthesized via chemical solution approach. The chemicals such as the nitrate salt of zinc, hexamethylenetetramine and NaOH were utilized and the acquired solution was refluxed at ~90 °C for 60 min for fabrication of nanorods. Thereafter, the obtained NRs were well characterized with the instruments such as X-ray diffraction pattern (XRD), field emission scanning electron microscopy (FESEM), transmission electron microscopy (TEM) and Fourier transform infra-red (FTIR) spectroscopy also with electrochemical data. The well crystalline nanorods were used as an electrode material for to high sensitive hydrazine sensor detection with glassy carbon electrode (GCE). The cyclic voltammetry (CV) data's were analyzed from low (2μL/100 mL PBS) to high concentration (1–5 mL/PBS) of hydrazine with NRs/GCE electrode. The electrochemical impedance spectroscopy (EIS) was evaluated from 0 to 5 mL of solution at 4211 Z/ohm conditions. The proposed sensor and their stability are the promising features of the sensor.

1. Introduction

Any society is directly or indirectly affected with the pollution, especially environmental, which is a major apprehension. The environment is polluted with the release of various chemical effluents, directly contaminated and causes an adverse effect to the whole biota [1,2]. Over various organic and inorganic pollutants, hydrazine (N_2H_4) has attracted significant attention of the scientific community due to their significance in the industries for instance agriculture, pharmacy, military, fuels, aerospace, catalysis and so on [3–5]. The application of hydrazine (N_2H_4) chemical in industry for various purposes such as it reduces the corrosion, applies as pharmaceutical intermediates, catalysts, emulsifiers, antioxidants, insecticides, herbicides, pesticides, dyestuffs, and explosive etc [1–6]. However, it is a toxic, carcinogenic and hepatotoxic material, which causes adverse effects on human health, irritation of eyes, nose and throat, temporary blindness, dizziness, nausea, pulmonary edema, coma, blood abnormalities, severe damage to liver, lungs, kidneys, DNA and human central nervous system [7]. Because of the wider application in industry and directly related to public health, it is obvious and mandatory to form a reliable, rapid and highly sensitive senor for the detection and determination of hydrazine concentration/level in the environment. Towards this direction, the techniques such as electrochemical, chromatographic and spectroscopic is reported in the literature [8–11]. Among them, the electrochemical technique is promising, portable, economical, robust and high-sensitive towards the determination of hydrazine [12]. Although the electrochemical studies are quick, reliable and reproducible but the main challenge is to design the nanostructured materials for sensing application with high efficiency and active electron transport medium at an electrode. In this direction, the nano-structured materials, which exhibit good optical, electrical and high surface properties, have possibility to change and give high output of electron transport properties. The electro-chemical property of hydrazine is slow and it requires high potential with working electrodes. To accelerate the rate of oxidation and reduce the over potential, many attempts have been adopted for to develop the electron mediator species for detection of hydrazine, for instance nanoparticle [13–17] and complexes [18,19]. The organized and zero dimensional sphere shaped nanostructures exhibit the property to increase the electron transfer rate due to their organization and high surface area [19,20]. It is required to select the best geometrical nanostructures, which is the key factor for the sensitization of hydrazine sensor. Several electrodes have been developed based on nanostructured material for the detection of hydrazine for instance PEG coated nano zinc sulfide were formed by Mehta et al. [21] and achieve best sensitivity (~89.3 μAuM^{-1}) for their fabricated electrode [21]. Umar et al. reported the fabrication of sea-urchins prepared hydrothermally (at 165°C) and used as an electrode material for the detection of phenyl hydrazine from 0.0 to +1.5V *via* I–V

* Corresponding author. College of Science, Department of Zoology, P.O. Box 2455, King Saud University, Riyadh, 11451, Saudi Arabia.
E-mail addresses: rwahab05@gmail.com, rwahab@ksu.edu.sa (R. Wahab).

https://doi.org/10.1016/j.vacuum.2019.04.036
Received 23 February 2019; Received in revised form 15 April 2019; Accepted 16 April 2019
Available online 17 April 2019
0042-207X/

technique [22]. The zinc oxide nanocones were used to check the electrochemical detection against hydrazine and sensitivity was observed $50 \times 10^4\ \mu A\ cm^{-2}\ \mu M^{-1}\ cm^{-2}$ with the limit of detection range is 0.01 mM [23]. The composite material of zinc oxide and SiO_2 was also detected similarly and formed a sensor which is to be 1.42 μM with sensitivity and it reaches to $10.80\ \mu A\ cm^{-2}\ mM^{-1}$ [24]. In this continuation, the silver doped zinc oxide nanorods sensitivity was acquired $105.5\ \mu A\ \mu M^{-1}\ cm^{-2}$ with the concentration of 98.6 mM with sensor detection limit was 5×10^{-2} mM [25]. In other report, Fe_2O_3 based carbon nanocomposite electrode were fabricated and they have succeeded the sensitivity of $\sim 0.0445\ \mu A \mu M^{-1}$ [26]. The nanocopper oxide and nanoarray's structured were also empl-oyed to fabricate as a hydrazine based sensor and to attain $29.78\ \mu A \mu M^{-1}$, $\sim 94.21\ \mu A \mu M^{-1}$ sensitivity respectively [21,27]. Including the oxide material the metal nanoparticles such as palladium nanoparticles decorated with cobalt nanoparticles (CoNPs), enfolded with carbon nanotubes (Pd/Co-NCNTs) in nitrogen atmosphere were utilized for the detection of hydrazine as an amperometric sensor [28]. In another report, the doped material Fe_2O_3/CeO_2 nanocubes (NCs), were applied on a glassy carbon electrode (GCE) and used as film form chemical sensors detect the hydrazine level via the electrochemical method [29]. The nanoparticles of ZnO were also used as an electrode material pasted on glassy carbon electrode (GCE) and tested for to utilize as a working electrode for the detection of hydrazine [30]. The fluorescent N_2H_4 probes are different type's shows the sensing mechanism and these probes designing process are comprehensively explained on aspects of unique chemical characteristics of N_2H_4 and the structures with spectral properties of fluorophores [31,32].

Over various types of electrodes prepared through different materials, the zinc oxide based nanostructures, which has a special attraction because of their versatile properties such as wide band gap energy (3.37eV), high exciton binding energy (60 meV), high thermal stability, good volume to surface etc makes an excellent and distinct material [33,34]. Due to their outstanding and versatile properties of ZnO nanostructures, it has been used in various high-technological applications such as dye-sensitized solar cells (DSSCs), field effect transistors, field emission devices (FEDs), p-n-heterojunction diodes, sensors (chemical, bio and gas) and UV-detectors [35–39]. Besides these, the zinc oxide nanostructures which have unique bio-compatible and non-toxic nature, attracted researchers for the fabrication of chemical and biological sensors including hydrazine based sensor. The biocompatible property facilitates more and more ways for the immobilization and surface attachment of biomolecules [40–47].

The present work displays the synthesis of hexagonal shaped zinc oxide nanorods via chemical solution process. The formed hexagonal nanorods (NRs) were characterized via XRD to examine the crystalline character of the material whereas the structural dimensions were measured via FESEM and TEM consequently. To know the functional and chemical characteristic of the prepared material, were analyzed via FTIR. The formed electrode materials oxidation and reduction potential attached on GCE were measured by CV at low, mid and high concentration levels of hydrazine in PBS (phosphate buffer solution). Apart from this the EIS was also checked and evaluated for the formed electrode at low and high concentration of the hydrazine solution.

2. Experimental

2.1. Materials and methods

2.1.1. Preparation of ZnO nanorods (ZnONRs)

The synthesis of nanostructures in the form of powder was accomplished with using chemicals such as nitrate salt of zinc ($Zn(NO_3)_2.6H_2O$), sodium hydroxide (NaOH) and hexa methylenetetramine ($(CH_2)_6N_4$, HMT). The chemicals were procured from Aldrich Chemical Corporation and used as received. For the preparation of nanopowder, about ~ 0.3 M of nitrate salt of zinc and a HMT (4.9×10^{-2} M) were mixed in 100 mL of double distilled water (DDW) and stirred the solution of 30 min and the pH was checked which reaches to 6.3. When the solution was completely mixed, NaOH (3 M) was added to this solution gradually to enhance the solutions basic condition and their pH was lifted to 12.5. For few seconds a white colored suspension was appeared in the beaker and then changes to original condition. The solution was moved to a glass pot (~ 250 mL capacity) and refluxed at 90 °C for an hour. At initial no change was examined whereas when the temperature roses, imagine that initial formation of nanorods were started and this heating was continued and completed in an hour. After the complete reaction, the glass pot was cooled at room temperature, washed with organic solvents and dried. The white powder was analyzed for their crystalline, structural and electrochemical studies.

2.1.2. Characterization of zinc oxide nanorods

The materials phases were characterized via XRD (PANanalytical Xpert Pro., United Kingdom) with $Cu_{K\alpha}$ radiation (1.54178 Å) ranges from 20 to 80° with 6°/min rotation. The shape and size of the nanostructures were examined via FESEM (Hitachi S-4700, Japan).

The structural detail was further examined for the prepared powder by using TEM (JEOL JEM JSM 2010; Hitachi Japan) operated with an acceleration voltage of 200 kV at room temperature. The obtained powder was dissolved in an ethanol (EtOH) solvent and sonicated in a bath sonicator (~ 40 W) for ~ 10 min, and to this suspension solution a copper grid (~ 400 mesh, Sigma) was dipped for about 1–2 min and removed from the solution. The copper grid was dried at room temperature, and fixed it to the sample holder for structural analysis. The functional characteristic of the prepared powder was observed via FTIR (FTIR; Perkin Elmer-FTIR Spectrum-100, U.S.A.) in the range of 400–4000 cm^{-1} with KBr powder.

2.1.3. Hydrazine sensor based with hexagonal ZnO nanorods

The prepared hexagonal shaped nanostructures were applied as an electron mediator/working electrode to sense the N_2H_4. To make a sensor fabrication, the ZnONRs were coated as film form on GCE electrode with an active surface area (SA = 0.071 cm^2). For coating, the small amount of NRs of zinc oxide was mixed with butyl carbitol acetate (BCA) in a specified ratio (70:30 ratio) and the prepared slurry was coated on GCE electrode, dried at 60 ± 5 °C for 30–45 min to get a uniform layer over entire electrode surface. The electrochemical performance of the prepared electrode were studies via Autolab Potentiostat/galvanostat, PGSTAT 204-FRA32 control with NOVA software (Metrohom Autolab B.V.Kanaalweg 29-G, 3526 KM Utrecht, Netherlands) in three electrode system [47,48]. The prepared NRs based zinc oxide/GCE electrode was used as a working electrode; to this a platinum (pt) wire was used as a counter electrode whereas Ag/AgCl (sat.KCl) was employed as a reference electrode. The PBS (0.1 M; pH 7.2) with hydrazine was used as an electrolyte solution for all electrochemical measurements. To sense the hydrazine concentration with ZnONRs/GCE, an inclusive range of hydrazine (2 μL–10μL/100 mL PBS and 1 mL–5 mL/100 mL PBS) with −0.2 to +2.0 V current was adopted to determine the sensing characteristics. The sensitivity and amperometric response with current-time (i-t) curves were measured at a potential of 0.5 V in PBS solution. To know the exposure of real sample, 10 μL of hydrazine was added to 100 mL PBS solution.

2.1.4. Electrochemical impedance spectroscopy (EIS) measurements

The EIS were employed to examine the prepared ZnONRs/GCE electrode with the wide range of hydrazine concentrations (1 mL–5 mL/100 mL PBS) with frequency range, 10 kHz–0.01 Hz.

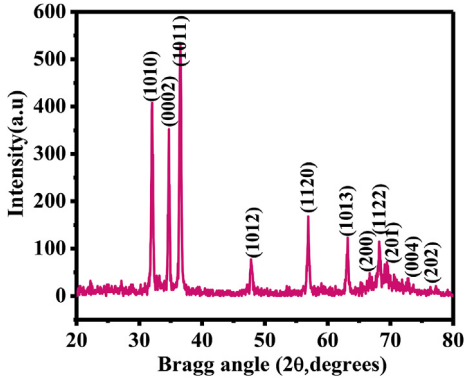

Fig. 1. Typical X-ray diffraction pattern of zinc oxide nanorods (ZnO-NRs).

3. Results and discussion

3.1. X-ray diffraction result of prepared powder

The size, phase and crystalline character of the prepared white powder were analyzed via the XRD pattern from the range of 20–80° with 6°/min scanning speed at room temperature. The acquired data clearly demonstrates that almost all peaks and their positions (<1010> (31.95), <0002> (34.70), <1011> (36.60), <1012> (47.80), <1120> (56.90), <1013> (63.20), <200> (66.70), <1122> (67.65), <201> (68.20), <004> (72.30) and <202 > (76.65)) are analogous with the available powder diffraction data JCPDS 36–1451 and lattice constants a = 3.249 and c = 5.206 Å (Fig. 1). The obtained data reveals that the prepared powder is crystalline in nature and correspondents to the wurtzite phase of commercial powder of ZnO. The spectrum defines no such peak was examine except ZnO, further indicates that the prepared structure is pure ZnO [48].

3.2. Morphological evaluation of nanopowder/prepared powder

The morphology of the processed structure in the form of white powder was analyzed via FESEM and achieved data is represented as Fig. 2. The image (Fig. 2a and b) shows that many rod shaped structure nanostructures with high density and in larger areas are seen in the image, where some are combine with other one and some are seen individual. When the structure was analyzed at high magnified or clearer observation (Fig. 2c and d), it shows that the individual rods are having hexagonal structure, are about 200–250 nm in diameter whereas the size goes up to 3–4 μm (Fig. 2d). From the observation the prepared nanostructures are exhibit smooth surfaces, with full hexagonal morphology and are appeared in the images. For further confirmation of morphology of the structures, powder was analyzed with TEM at 200 kV. Fig. 2e shows the low magnified TEM image of obtained nanorods, the data is close related to the FESEM observation and are clearly consistent. The crystalline property and distance of lattice fringes were examined through HR-TEM, which discloses that the nanorods are highly crystalline and having lattice distance is about 0.526 nm separately (Fig. 2f) and this is identical to wurtzite ZnO. From the obtained observation express that the nanorods are favorably grows along the c-axis [0001] direction (Fig. 2f).

3.3. Functional characterization (FTIR spectroscopy)

As described in experimental section, the FTIR spectroscopy was evaluated with KBr in the ranges from 4000 to 400 cm^{-1}. Fig. 3. Illustrates a wide peak obtained in the range of 3200–3600 cm^{-1} signifies the stretching mode of vibration in hydroxyl group (O—H) [48]. Very small peak at 2300–2400 denotes the atmospheric CO_2. The sharp peak at 1457 cm^{-1} shows the bending mode of vibration in water (HOH) [18,20] molecule. The symmetric and asymmetric stretching modes of vibration for nitro group were also observed at 1065 and 885 cm^{-1}. The peak at 493 cm^{-1} denotes the metal oxide peaks. The functional change in the material states that the hydroxide molecules changes to metal oxides [48] (Fig. 3).

3.4. Electrochemical studies (CV) results

The prepared modified working electrode based on hexagonal zinc nanorods (area 2 × 2 cm^2) on ZnO-NRs/GCE was checked in absence and presence of hydrazine (10 μL) in 100 mL of PBS (0.1 M, pH 7.2) solution with the scan rate of 100 mV/s. From the obtained spectra, it can be seen that good activity for hydrazine oxidation [2]. As can be seen from the spectra, the set potential (0.65 V) for hydrazine solution [3] was moved to less value with and without hydrazine solution (1.1 V), the spectra, confirms that the prepared modified electrode based on ZnO-NRs/GCE is much efficient for the transport of electron and oxidize the hydrazine [1] solution (Fig. 4).

3.5. Effect of hydrazine concentration on modified electrode (ZnO-NRs/GCE)

To evaluate the routine investigation of current and potential (I—V) for the modified ZnO NRs/GEC with different concentration (2, 4, 6, 8 and 10 μL) of hydrazine electrolyte in 100 mL PBS and the obtained result is presented as Fig. 5. The stock solution of hydrazine was prepared for the study of different concentration of hydrazine in PBS solution. To evaluate the routine investigation of current and potential (I—V) for the modified - ZnONRs/GEC with innumerable concentration of hydrazine in 100 mL PBS and presented as Fig. 5. The stock solution of hydrazine was prepared for the study of different concentration of hydrazine in PBS solution. The obtained spectrum represents at low range of hydrazine concentration solution, and this was examined at 100 mV with current potential ranges from −1.5 to 1.5 V. As can be seen that current at anodic peak is directly related to the hydrazine concentration and it increases with the increase of concentration of hydrazine in the PBS solution. It assumed that when the current in the form of ions (hydrazine and hydroxyl) increases with the increase of hydrazine concentration which resembles to the fast electrons transfer on to the conduction band. A high potential of anodic peak was also observed from another experiments, when hydrazine was used at high concentration level (1–5 mL). The electron was displaced due to the increased amount of hydrogen ions in the solution (Fig. 6).

3.6. Influence of scan rates

For more detail related to the scan rate and catalytic reactions between the hydrazine and modified ZnONRs on GCE electrode, which involved in the sensing process at various scan rates (5, 10, 20, 50 and 100 mVs^{-1}) were evaluated and presented as Fig. 7. The scan rate exhibit that the peak currents increase on increasing the scan rate, in 0.1 M PBS solution, confirms that the oxidation process is diffusion controlled. For more detail related to the scan rate and catalytic reactions between the hydrazine and modified ZnO NRs on GCE electrode, which involved in the sensing process at various scan rates (5, 10, 20, 50 and 100 mVs^{-1}) were evaluated and presented as Fig. 7. The scan rate exhibit that the peak currents increases on increasing the scan rate, in 0.1 M PBS solution, confirms that the oxidation process is diffusion controlled. A successive response at different scan rate of hydrazine of 0.1 M PBS solution of pH 7.2 was observed and presented as Fig. 7. The enhancement in current was observed after at various scan rates (5, 10, 20, 50 and 100 mVs^{-1}). From the obtained graph and it can be concluded and show the relation between the current and potential enhancement of fabricated hydrazine sensor (Fig. 7).

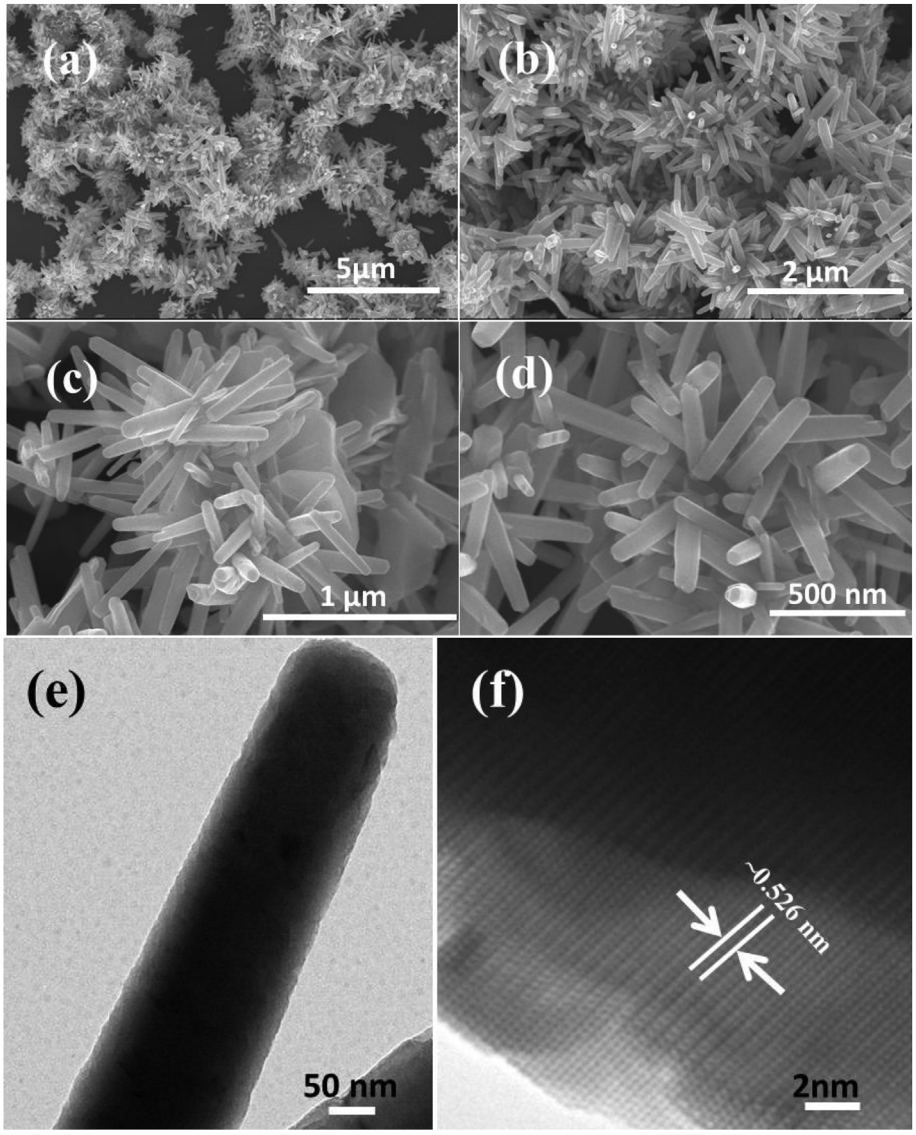

Fig. 2. FESEM images of ZnO-NRs: (a–b) shows the low magnification images and (c and d) show the high magnification image of ZnO-NRs. whereas (e) shows the low magnification TEM image of ZnO-NRs and (f) presents the HR-TEM image and it shows the lattice difference between two fringes is about ~0.526 nm with the ideal fringes distance.

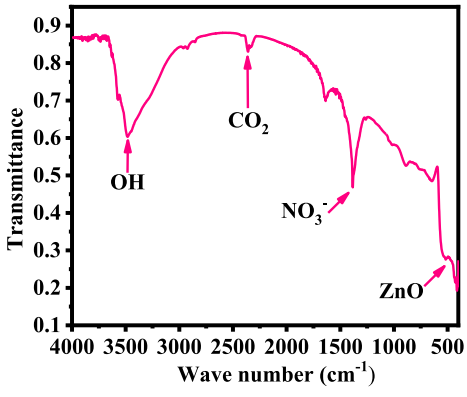

Fig. 3. Typical FTIR spectrum of grown ZnO-NRs.

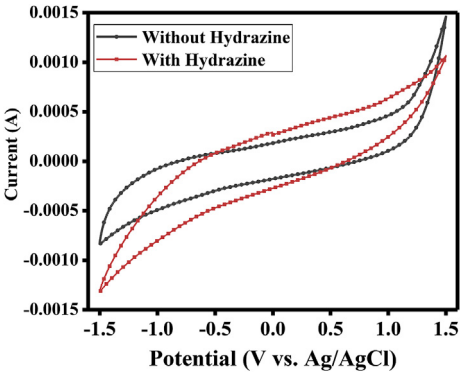

Fig. 4. Typical I − V response of ZnO NRs based GCE in absence and presence of hydrazine at scan rate of 100 mV/s.

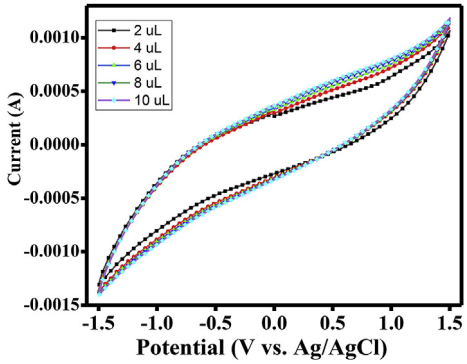

Fig. 5. (a) Typical I − V response of ZnO NRs based GCE at low range concentrations (from 2 μL to 10 μL) of hydrazine into 0.1 M PBS solution (pH7.2). The scan rate is 100 mV/s (b) Linear calibration plot obtained using CV data for ZnO NRs based GCE.

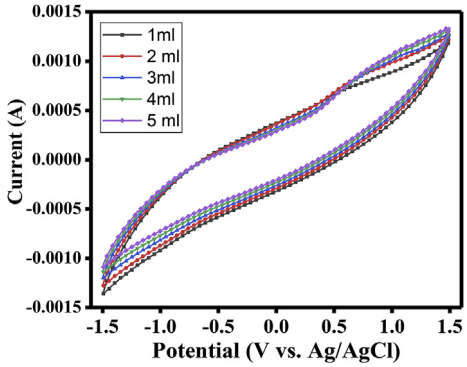

Fig. 6. Typical I − V response of ZnO NRs based GCE at various high concentrations (from 1 mLto 5 mL) of hydrazine into 0.1 M PBS solution (pH 7.2).

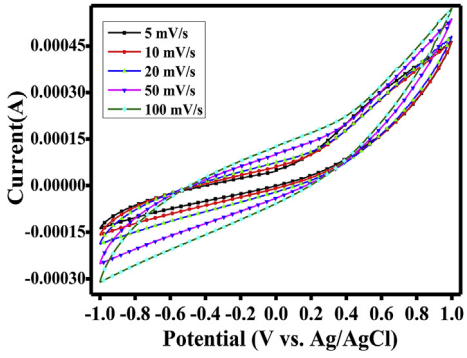

Fig. 7. CV obtained for ZnONRs based GCE at in 0. 1 M PBS containing hydrazine solutions at various scan rates 5, 10, 20, 50 and 100 mVs^{-1} with −1.0 to +1.0 potential.

3.7. Influence of time response

To know the prepared sensor selectivity and reproducibility, the time response was also measured from 0 to 600 s (Fig. 8). A sequential time response was observed at different time span for the prepared ZnONRs/GCE based hydrazine sensor. At 100s not much response was observed in the current whereas as the time span increases at 200s, 300s, 400s, 500s and 600s current enhances to 9.436×10^{-6}, 1.442×10^{-5}, 2.030×10^{-5}, 2.789×10^{-5} consequently for the prepared electrode. The obtained data states that the produced sensor is specific, selective, and reproducible and exhibits enough sustainability for long time.

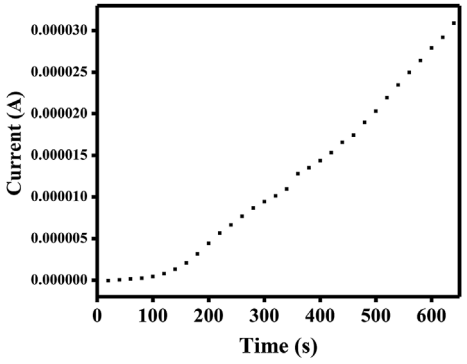

Fig. 8. Amperometric response of ZnO NRs based GCE with successive addition of hydrazine into 0.1 M PBS buffer solution (pH 7.0), which depicts the time (0–650 s) and current spectra for the reliability and reproducibility of the optimized data.

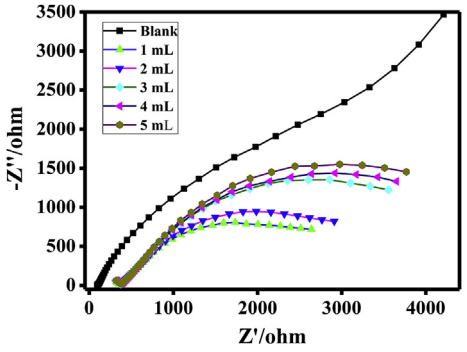

Fig. 9. Electrochemical impedance spectra of ZnO NRs modified GCE towards various high concentrations (from 1 mL to 5 mL) of hydrazine into 0.1 M PBS solution (pH 7).

3.8. Electrochemical impedance spectroscopy (EIS) studies

The EIS measurement was used to know the ion transport (hydrazine and hydroxyl) mecha nism/internal resistance between the electrode and the electrolyte (varied concentration of hydrazine loadings) for the fabricated ZnONRs/GCE electrode in frequency range from 0.01 Hz to 10 kHz and the result presented as Fig. 9. In Nyquist plot, Z′ represents the ohmic property and -Z″ represents the capacitive property. The impedance behavior is generally dominated by three major process occurring in the high, medium and low frequency region, respectively. The obtained wide semicircle curve of electrochemical impedance of the smaller curve corresponds to a smaller charge transfer resistance. The present case indicates that the wide semicircle which is in the high-frequency region was observed and it resembles to electron-transfer limited process. The high-frequency region in diameter of the semicircle corresponds to the charge transfer resistance ((R_{ct}) and controls electron transfer kinetics of the redox probe at electrode/electrolyte interface. It's well known that a larger semicircle curve represent a high interfacial charge transfer resistance, which probably results from the poor electrical conductivity of the active materials. From the obtained curve in Fig. 9, shows that diameters of the semicircle at low hydrazine concentrations are much smaller than the high concentrations due to less charge transfer resistance in the fabricated electrode [49–51].

3.9. Possible mechanism

The synthesized hexagonal shaped zinc oxide nanorods (ZnO-NRs), which is a semiconductor material and exhibit good band gap (3.37 eV), plays an important role to enhance the electroactive properties due to

their number of active sites for and higher surface properties [52]. The larger range of electrochemical detection of hydrazine (analyte) at low (10–100 μL), median (0.1–1 mL/100 mL PBS) and high (1–5 mL/100 mL PBS) concentrations were evaluated in this experiment. The GCE/ZnO-NRs based electrode develops as an active material for the electrochemical sensing of hydrazine for larger utilities in industries and also for the environmental studies [53]. The developed electrochemical sensor works on the principle of variation in concentration of analyte (hydrazine) and their adsorption and conductance on zinc oxide nanorods (ZnO-NRs) based on GCE electrode. In this experiment, the atmospheric oxygen, which has an ability to physisorbed on the surface of nanostructured based electrode (ZnO-NRs) and this oxygen molecule can be possible to move from site to site and ionized (O^{-}_{ads}) through the elimination of electron from the conduction band then convert into their oxidized form (O^{-} or O^{2-}) on the surface of nanorods layer, which form a charge layer between surface layer of nanostructures and analyte [48,54]. This amplifies the potential and enhanced the resistance of the developed sensor, which leads a decrease in the conductance of sensor and increase in potential. On the basis of the acquired data and their analysis, it represents that due to the presence of hydrazine molecule (analyte) the prepared nanobased film enhanced the conductivity. It also imagines that at higher concentration of analyte provides higher efficiency, which upsurged the resistivity. In our experiment, we have tested from very low hydrazine (analyte) concentration to higher concentration, which illustrates from CVs results. It's well conventional that the sensor results affect, on the basis of their organization of selected nanostructured material such as nanorods, nanoflowers, nanoparticles, their properties, ways applied for their synthesis etc. The studies shown that the nanorods found higher sensing aptitude as compared to others nanostructures because of their structural symmetry. The ZnO nanostructures/molecules have a tendency to generate a constructive environment on their surfaces, which facilitates the assessment of hydrazine molecule (analyte) via adsorption process. The higher sensitivity, stability and better reproducibility with zinc oxide based nanostructures endorsed the enhanced rate of electron transportation between the zinc oxide based nanostructures film, which works as an electrode and hydrazine molecule are their addition assets. The surface immobilization affects the response time and performance of the developed sensor, which can be improved via the proper use of catalyst and spill to the whole surface of the developed electrode. The catalyst exhibits the possibility to enhance the reaction with pre-adsorbed surface oxygen of the material, increase the conductance and response of the prepared electrode [25,48,53,54].

4. Conclusions

The conclusion of the present work states that the hexagonal shaped nanorods were formed via solution process with use zinc nitrate hexa hydrate ($Zn(NO_3)_2.6H_2O$), sodium hydroxide (NaOH) and hexamethylamine ($(CH_2)_6N_4$, HMT), in a very less time (60 min) span and were characterized well in terms of their structural, chemical and electrochemical studies. The processed materials were initially characterized in terms of structural and chemical properties via the XRD, to examine the crystalline properties whereas the morphology of nanorods were accessed through FESEM and it reveals that the individual rod size is in the range of 3–4 μm (length) and diameter ranges about 200-250 nm. The obtained dimensional value was also confirmed from TEM and is consistent with the FESEM. The nanorods were applied as an efficient nanosensor against the catalyst N_2H_4 chemical sensor. The CV was applied to know the ionic exchange in a liquid medium from very low (2 μL N_2H_4/100 mL PBS) to high concentration (5 mL/100 mL PBS) with hydrazine solution were observed. A sequential change in the oxidation and reduction peaks were examined which indicates that the obtained sensor is specific and can be useful for the large scale detection. The obtained sensors are selectivitve, reproducible andwere observed from zero to 600 s deals that it exhibit enough sustainability for longer period. Including this, EIS defines the good contact of the prepared electrode with electrolyte and electrode with in the specified frequency range (0.01 Hz–10 kHz).

Conflicts of interest

The authors declare that there are no conflicts of interest.

Acknowledgement

The authors extend their appreciation to the Deanship of Scientific Research at King Saud University for funding this work through research group no. RG-218.

References

[1] S.D. Zelnick, D.R. Mattie, P.C. Stepaniak, Occupational exposure to hydrazines: treatment of acute central nervous system toxicity avait, Space Environ. Med. 74 (12) (2003) 1285–1291.
[2] K. Yamada, K. Yasuda, N. Fujiwara, Z. Siroma, H. Tanaka, Y. Miyazaki, T. Kobayashi, Potential application of anion-exchange membrane for hydrazine fuel cell electrolyte, Electrochem. Commun. 5 (2003) 892.
[3] J.W. Mo, B. Ogorevc, X. Zhang, B. Pihlar, Cobalt and copper hexacyanoferrate modified carbon fiber microelectrode as an all-solid potentiometric microsensor for hydrazine, Electroanalysis 12 (2000) 48–54.
[4] A. Umar, M.M. Rahman, S.H. Kim, Y.B. Hahn, Zinc oxide nanonail based chemical sensor for hydrazine detection, Chem. Commun. 2 (2008) 166–168.
[5] S. Garrod, M.E. Bollard, A.W. Nicholls, S.C. Connor, J. Connelly, J.K. Nicholson, E. Holm es, Integrated metabonomic analysis of the multiorgan effects of hydrazine toxicity in the rat, Chem. Res. Toxicol. 18 (2005) 115–122.
[6] W.X. Yin, Z.P. Li, J.K. Zhu, H.Y. Qin, Effects of NaOH addition on performance of the direct hydrazine fuel cell, J. Power Sources 182 (2008) 520–523.
[7] B.D. Morson, Evolution of cancer of the colon and rectum, Cancer 34 (1974) 845–860.
[8] K.M. Korfhage, K. Ravichandran, R.P. Baldwin, Phthalocyanine-containing chemi cally modified electrodes for electrochemical detection in liquid chromatography/flow injection systems, Anal. Chem. 56 (1984) 1514–1517.
[9] A. Savafi, M.A. Karimi, Flow injection chemiluminescence determination of hydrazine by oxidation with chlorinated isocyanurates, Talanta 58 (2002) 785–792.
[10] C.S. Leasure, G.A. Eiceman, Continuous detection of hydrazine and monomethyl hydrazine using ion mobility spectrometry, Anal. Chem. 57 (1985) 1890–1894.
[11] J. Wang, M. Chicharro, G. Rivas, X. Cai, N. Dontha, P.A.M. Farias, H. Shiraishi, DNA biosensor for the detection of hydrazines, Anal. Chem. 68 (1996) 2251–2254.
[12] K. Ravichandran, R.P. Baldwin, Liquid chromatographic determination of hydrazines with electrochemically pretreated glassy carbon electrodes, Anal. Chem. 55 (1983) 1782–1786.
[13] K.I. Ozoemena, T. Nyokong, Electrocatalytic oxidation and detection of hydrazine at gold electrode modified with iron phthalocyanine complex linked to mercaptopyridine self-assembled monolayer, Talanta 67 (2005) 162–168.
[14] S.V. Guerra, C.R. Xavier, S. Nakagaki, L.T. Kubota, Electrochemical behavior of copper porphyrin synthesized into zeolite cavity: a sensor for hydrazine, Electroanalysis 10 (1998) 462–466.
[15] S.J.R. Prabakar, S.S. Narayanan, Amperometric determination of hydrazine using a surface modified nickel hexacyanoferrate graphite electrode fabricated following a new approach, J. Electroanal. Chem. 617 (2008) 111–120.
[16] M.R. Majidi, A. Jouyban, K. Asadpour-Zeynali, Electrocatalytic oxidation of Hydrazine at overoxidized polypyrrole film modified glassy carbon electrode, Electrochim. Acta 52 (2007) 6248–6253.
[17] A. Salimi, L. Miranzadeh, R. Hallaj, Amperometric and voltammetric detection of hyd razine using glassy carbon electrodes modified with carbon nanotubes and catechol derivatives, Talanta 75 (2008) 147–156.
[18] G.Y. Gao, D.J. Guo, C. Wang, H.L. Li, Electrocrystallized Ag nanoparticle on functional multi-walled carbon nanotube surfaces for hydrazine oxidation, Electrochem. Commun. 9 (2007) 1582–1586.
[19] B.M. Christopher, E.B. Craig, O.S. Andrew, G.J.J. Timothy, R.G. Compton, The electro analytical detection of hydrazine: a comparison of the use of palladium nanoparticles supported on boron-doped diamond and palladium plated BDD microdisc array, Analyst 131 (2006) 106–110.
[20] C. Wang, L. Zhang, Z. Guo, J. Xu, H. Wang, K. Zhai, X. Zhuo, A novel hydrazine electrochemical sensor based on the high specific surface area graphene, Microchim. Acta 169 (2010) 1–6.
[21] S.K. Mehta, Khushboo, A. Umar, Highly sensitive hydrazine chemical sensor based on mono-dispersed rapidly synthesized PEG-coated ZnS nanoparticles, Talanta 85 (2011) 2411–2416.
[22] A. Umar, M.S. Akhtar, A. Al-Hajry, M.S. Al-Assiri, G.N. Dar, M.S. Islam, Enhanced photocatalytic degradation of harmful dye and phenyl hydrazine chemical sensing using ZnO nano-urchins, Chem. Eng. J. 262 (2015) 588–596.
[24] S. Kumar, G. Bhanjana, M. Dilbaghi, A. Umar, Zinc oxide nanocones as potential scaff old for the fabrication of ultra-high sensitive hydrazine chemical sensor, Ceram. Int. 41 (2015) 3101–3108.
[23] A.M. Ali, F.A. Harraz, A.A. Ismail, S.A. Al-Sayari, H. Algarni, A.G. Al-Sehemi,

Synthe- sis of amorphous ZnO–SiO2 nanocomposite with enhanced chemical sensing pro perties, Thin Solid Films 605 (2016) 277–282.
[25] S. Chaudhary, A. Umar, K.K. Bhasin, S. Baskoutas, Chemical sensing applications of ZnO nanomaterials, Materials 11 (2018) 287, https://doi.org/10.3390/ma11020287.
[26] B. Sljukic, C.E. Banks, A. Crossley, R.G. Compton, Iron (III) oxide graphite compo site electrodes: application to the electroanalytical detection of hydrazine and hydrogen peroxide, Electroanalysis 18 (2006) 1757–1762.
[27] Z. Yin, L. Liu, Z. Yang, An amperometric sensor for hydrazine based on nano-copper oxide modified electrode, J. Solid State Electrochem. 15 (2011) 821–827.
[28] Y. Zhang, B. Huang, J. Yeb, J. Ye, A sensitive and selective amperometric hydrazine sensor based on palladium nanoparticles loaded on cobalt-wrapped nitrogen-doped carbon nanotubes, J. Electroanal. Chem. 801 (2017) 215–223.
[29] M.M. Rahman, M.M. Alam, A.M. Asiri, Selective hydrazine sensor fabrication with facile low-dimensional Fe2O3/CeO2 nanocubes, New J. Chem. 42 (2018) 10263–10270.
[30] J. Deng, S. Deng, Y. Liu, Highly sensitive electrochemical sensing platform forHydrazine detection, Int. J. Electrochem. Sci 13 (2018) 3566–3574.
[31] K.H. Nguyen, Y. Hao, W. Chen, Y. Zhang, M. Xu, M. Yang, Y.N. Liu, Recent progress in the development of fluorescent probes for hydrazine, Luminescence 33 (5) (2018) 816–836.
[32] G. Wang, A. Gu, W. Wang, Y. Wei, J. Wu, G. Wang, X. Zhang, B. Fang, Copper oxide nanoarray based on the substrate of Cu applied for the chemical sensor of hydrazine detection, Electrochem. Commun. 11 (2009) 631–634.
[33] A. Umar, S.H. Kim, Y.S. Lee, K.S. Nahm, Y.B. Hahn, Catalyst-free large-quantity synth esis of ZnO nanorods by a vapor–solid growth mechanism: structural and optical properties, J. Cryst. Growth 282 (2005) 131–136.
[34] A. Umar, S.H. Kim, H. Lee, N. S Lee, Y.B. Hahn, Optical and field emission pro perties of single-crystalline aligned ZnO nanorods grown on aluminium substrate, J. Phys. D Appl. Phys. 41 (2008) 065412.
[35] T.W. Hamann, A.B.F. Martinson, J.W. Elam, M.J. Pellin, J.T. Hupp, Aerogel templated ZnO dye-sensitized solar cells, Adv. Mater. 20 (2008) 1560–1564.
[36] W.I. Park, J.S. Kim, G.-C. Yi, M.H. Bae, H. J Lee, Appl. phys. lett., fabrication and electrical characteristics of high-performance ZnO nanorod field-effect transistors, 85 (2004) 5052–5054.
[37] C.S. Rout, A.R. Raju, A. Govindaraj, C.N.R. Rao, Hydrogen sensors based on ZnO nanoparticles, Solid State Commun. 138 (3) (2006) 136–138.
[38] T.-H. Moon, M.-C. Jeong, W. Lee, J.-M. Myoung, The fabrication and characterization of ZnO UV detector, Appl. Surf. Sci. 240 (1–4) (2005) 280–285.
[39] Y. Huang, Y. Zhang, Y. Gu, X. Bai, J. Qi, Q. Liao, J. Liu, Field-emission of a single In-doped ZnO nanowire, J. Phys. Chem. C 111 (2007) 9039–9043.
[40] A. Umar, M.M. Rahman, Y.B. Hahn, Ultra-sensitive hydrazine chemical sensor based on high-aspect-ratio ZnO nanowires, Talanta 77 (2009) 1376–1380.
[41] K.B. Lee, K.S. Cho, H. Kwon, Morphological transition of vertically aligned one-dimensional zinc oxide, Met. Mater. Int. 15 (2009) 649.
[42] W.I. Park, Controlled synthesis and properties of ZnO nanostructures grown by metal organic chemical vapor deposition: a review, Met. Mater. Int. 14 (2008) 659.
[43] Y. Qin, X.D. Wang, Z.L. Wang, Microfibre-nanowire hybrid structure for energy scavenging, Nature 451 (2008) 809–813.
[44] M. Yang, G.F. Yin, Z.B. Huang, X.M. Liao, Y.Q. Kang, Y.D. Yao, Well-aligned ZnO rod arrays grown on glass substrate from aqueous solution, Appl. Surf. Sci. 254 (2008) 2917–2921.
[45] N.G.N. Angwafor, D.J. Riler, Synthesis of ZnO nanorod/nanotube arrays formed by hydrothermal growth at a constant zinc ion concentration, Phys. Status Solidi 205 (2008) 2351.
[46] P.X. Gao, Y. Ding, W.J. Mai, W.L. Hughes, C.S. Lao, Z.L. Wang, Conversion of zinc oxide nanobelts into superlattice-structured nanohelices, Science 309 (5741) (2005) 1700–1704.
[47] F. Ahmed, S. Kumar, N. Arshi, M.S. Anwar, B.H. Koo, C.G. Lee, Rapid and cost effective synthesis of ZnO nanorods using microwave irradiation technique, Funct. Mater. Lett. 4 (1) (2011) 1–5.
[48] R. Wahab, N. Ahmad, M. Alam, A.A. Ansari, Nanocubic magnesium oxide: towards hydrazine sensing, Vacuum 155 (2018) 682–688.
[49] T. Mavrič, M. Benčina, R. Imani, I. Junkar, M. Valant, V.K. Iglič, A. Iglič, Chapter three - electrochemical biosensor based on TiO2 nanomaterials for cancer diagnostics, Adv. Biomembr. Lipid Self-Assem. 27 (2018) 63–105.
[50] P.P. Kumari, P. Shetty, S.A. Rao, Electrochemical measurements for the corrosion inhibition of mild steel in 1 M hydrochloric acid by using an aromatic hydrazide derivative, Arabian. J. Chem. 10 (5) (2017) 653–663.
[51] J. Wang, S. Yang, K. Zhang, A simple and sensitive method to analyze genotoxic impurity hydrazine in pharmaceutical materials, J. Pharm. Biomed. Anal. 126 (2016) 141–147.
[52] S.G. Ansari, R. Wahab, Z.A. Ansari, Y.S. Kim, G. Khang, A. Al-Hajry, Hyung-Shik Shin, Effect of nanostructure on the urea sensing properties of sol–gel synthesized ZnO, Sensor. Actuator. B 137 (2009) 566–573.
[53] J. Huang, C. Shi, G. Fu, P. Sun, X. Wang, C. Gu, Facile synthesis of porous ZnO micro belts and analysis of their gas-sensing property, Mater. Chem. Phys. 144 (2014) 343–348.
[54] M. Faisal, S.B. Khan, M.M. Rahman, A. Jamal, M.M. Abdullah, Fabrication of ZnOnanoparticles based sensitive methanol sensor and efficient photocatalyst, Appl. Surf. Sci. 258 (2012) 7515–7522.